Satellite-Based Photonic Quantum Networks Are Small-World

Samuraí Brito,[1] Askery Canabarro,[1,2] Daniel Cavalcanti,[3] and Rafael Chaves[1,4,*]

[1] *International Institute of Physics, Federal University of Rio Grande do Norte, Natal 59070-405, Brazil*

[2] *Grupo de Física da Matéria Condensada, Núcleo de Ciências Exatas—NCEx, Campus Arapiraca, Universidade Federal de Alagoas, Arapiraca-AL 57309-005, Brazil*

[3] *ICFO—Institut de Ciencies Fotoniques, The Barcelona Institute of Science and Technology, Castelldefels (Barcelona) 08860, Spain*

[4] *School of Science and Technology, Federal University of Rio Grande do Norte, Natal 59078-970, Brazil*

(Received 25 August 2020; accepted 15 December 2020; published 8 January 2021)

Recent milestone experiments establishing satellite-to-ground quantum communication are paving the way for the development of the quantum Internet, a network interconnected by quantum channels. Here, we employ network theory to study the properties of the photonic networks that can be generated by satellite-based quantum communication and compare them with those of their optical-fiber counterpart. We predict that satellites can generate small-world networks, implying that physically distant nodes are actually near from a network perspective. We also analyze the connectivity properties of the network and show, in particular, that they are robust against random failures. This positions satellite-based quantum communication as the most promising technology to distribute entanglement across large distances in quantum networks of growing size and complexity.

DOI: 10.1103/PRXQuantum.2.010304

I. INTRODUCTION

Quantum networks, distant nodes interconnected by quantum channels, are ubiquitous in quantum information science. Not only they can enhance our communication capabilities [1] but they also allow for a fundamentally secure quantum cryptography [2], the execution of quantum teleportation [3], the establishment of nonlocal correlations [4], and other applications such as clock synchronization [5] and quantum computation on the Cloud [6,7]. The two most promising infrastructures with which to build quantum networks are optical fibers and satellites [8]. Recent experimental advances [9–13] have allowed for quantum communication and the sharing of quantum entanglement over large distances, paving the way for the ongoing development of the quantum Internet [14–16].

Within this context, it becomes crucial to understand the network properties of a quantum Internet generated by these two technologies. For instance, the connectivity of the network (i.e.,, whether all nodes belong to the same network or if isolated islands of nodes exist) tells us whether it is possible to transmit information across the whole network. The network distance between nodes tells us how many entanglement swaps are needed if one wants to distribute entanglement between these nodes. Finally, the network robustness (i.e.,, how many nodes must be removed from the network until it breaks apart) informs us about how resilient the network is under local failures. In a recent study [17], we have shown that an optical-fiber-based network requires a very small density of nodes in order to produce fully connected photonic networks. However, the typical distances between nodes increase in a power-law relation with the number of nodes, i.e.,, the size of the network, meaning that it does not lead to the desired small-world property [18–22].

Here, we employ network theory [23] to study the properties of a satellite-based photonic network. Similarly to an optical-fiber-based quantum Internet (OFBQI), the satellite-based quantum Internet (SBQI) displays a transition from a disconnected to a connected network with respect to the density of nodes in the network. However, differently from an OFBQI, we observe the existence of hubs in a SBQI, i.e.,, nodes with a high number of connections, a phenomenon typically associated with scale-free networks [23]. Consequently, the SBQI leads to the small-world property, implying that very few entanglement swappings are necessary to distribute entanglement between any two nodes in the network. Moreover, similarly to the actual Internet [24,25], the SBQI also displays

*rchaves@iip.ufrn.br

a significant robustness against random failures in the network. On the down side, given the existence of hubs, it is less robust against targeted attacks, thus showing that highly connected nodes have to be specially protected in order to maintain the quantum network in an operative state.

II. NETWORK MODEL FOR THE SATELLITE BASED QUANTUM INTERNET

Formally, a network model is defined by a set of N nodes being connected by edges according to a given probabilistic rule. In our model (see Fig. 1), we assume that there is a satellite covering a disk of radius R, capable of connecting any two nodes within this area. More precisely, an entangled pair of photons is generated at the satellite and sent to each pair of nodes, via a down-link channel. The probability that a photon sent from the satellite arrives at site i has been analyzed in Ref. [26] and can be described by

$$p_{i,\mathrm{sat}} = \eta_0(1 - e^{2R_{\mathrm{rec}}^2/(w_{\mathrm{LT}}^i)^2}), \tag{1}$$

where $w_{\mathrm{LT}}^i \simeq 0,25 \times 10^{-5} d_{i,\mathrm{sat}}$ (for a down link) is the long-term beam width and depends on the distance $d_{i,\mathrm{sat}}$ between the site and the satellite; $\eta_0 \approx 0.1$ is an empirical factor [3] comprising the detection efficiency, the pointing losses, and the atmospheric attenuation; and R_{rec} is the radius of the telescope receptor (in our simulations, we consider $R_{\mathrm{rec}} = 0,75m$). The distance $d_{i,\mathrm{sat}}$ between site i and the satellite will depend on the position of the site within the coverage radius and the altitude h_{sat} of the satellite: that for the Micius satellite [27], used as reference here, is $h_{\mathrm{sat}} = 500$ km. Furthermore, we assume that the position of the satellite is fixed and positioned in the center of the disk. Finally, we will consider that the satellite can send n_p entangled pairs as an attempt to generate a link. A successful link is then established between sites i and j if at least one out of the n_p entangled pairs generated at the satellite arrives at the stations. This connection will happen with probability

$$\Pi_{ij} = 1 - (1 - p_i p_j)^{n_p}, \tag{2}$$

where $p_i \equiv p_{i,\mathrm{sat}}$ (similarly for p_j).

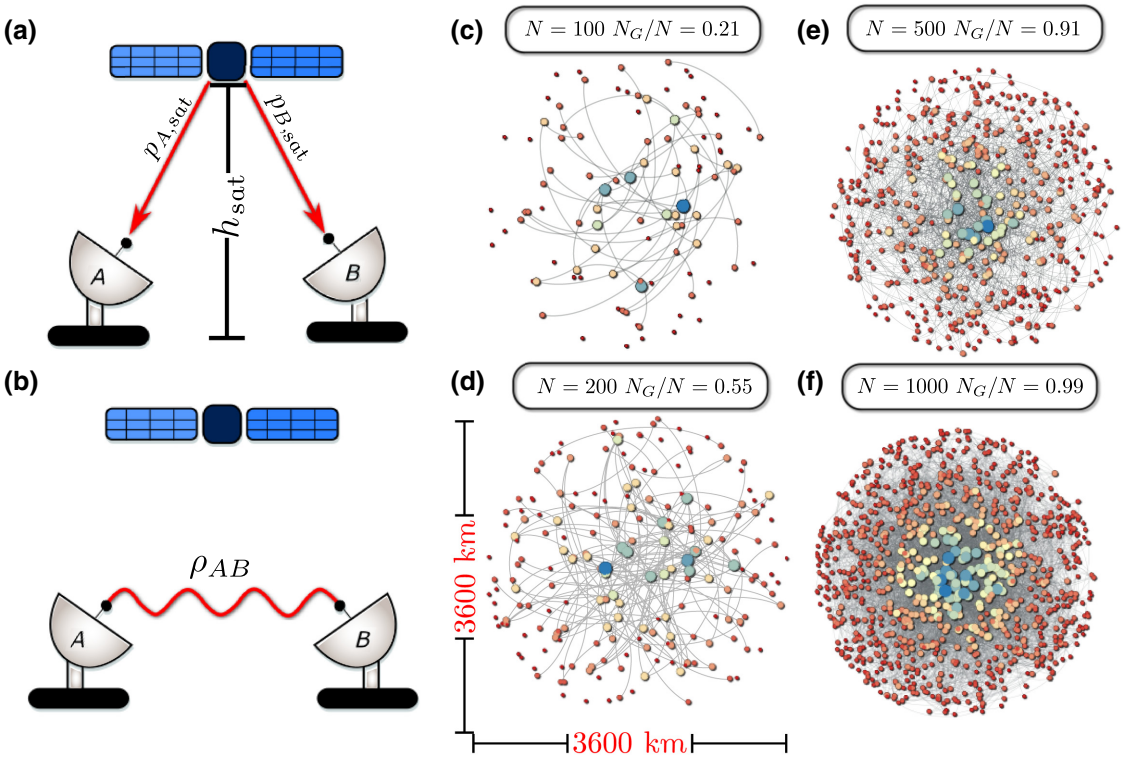

FIG. 1. Satellite-to-ground quantum communication and samples of the quantum Internet. (a) A satellite produces an entangled pair of photons and sends one photon to each station. The probability that each photon arrives at the destination is given by $p_{i,\mathrm{sat}}$. (b) A link between the two ground stations is formed when both photons arrive. (c)–(f) Samples from the quantum Internet. The gray edges represent the quantum link created by the satellite between two distant parts. The bigger (smaller) and bluish (reddish) the nodes, the more (less) connected they are. By increasing the number of nodes to (c) $N = 100$, (d) $N = 200$, (e) $N = 500$, and (f) $N = 1000$ in a fixed area of radius $R = 1800$ km, using $n_p = 50$ photons, the giant cluster will appear, i.e.,, the number of nodes within the largest cluster N_G is of the order of the total number of nodes N.

Within this framework, our model for the SBQI can be constructed in three steps:

1. N nodes are uniformly distributed in a disk of radius R (km).
2. We compute the Euclidean distance $(d_{i,\mathrm{sat}}, d_{j,\mathrm{sat}})$ between i and j and the satellite, for all pair of nodes i and j.
3. For each pair (i,j), we randomly sample a number uniformly distributed in the range $0 \leq r \leq 1$. If $r \leq \Pi_{ij}$, the sites are connected; otherwise, they are not.

To calculate the relevant properties of our network model in a statistically relevant manner, we use the standard Monte Carlo method up to 1000 steps to generate different instances of the SBQI model. In our simulations, we employ different values of the parameter n_p, observing that it does not change the qualitative properties of our model ($n_p = 50$ is chosen as a reference for the rest of the paper, unless stated otherwise). Examples of the generated networks are shown in Figs. 1(c)–1(f). As can be seen, even a few nodes in a large area can generate a network in a connected phase, i.e.,, $N_G \sim N$, where the variable N_G is defined as the number of nodes in the largest connected component (the giant cluster) and N is the size of the entire network [see Figs. 1(e) and 1(f)]. Another interesting feature is that, as the number of nodes increases, the most connected sites will naturally appear in the center of the disk (directly under the satellite). The further away from the center, the less connected the nodes are, which also means that the hubs are likely to appear in the center of the network area.

III. SATELLITE-BASED QUANTUM COMMUNICATION GENERATES SMALL-WORLD NETWORKS

A crucial property of a network that dictates most of its qualitative and quantitative properties is the connectivity distribution $P(k)$, i.e.,, the probability of finding a node with k connections. As shown in Fig. 2, we find that $P(k)$ can be well fitted by a log-normal distribution

$$P(k) = \frac{1}{k\sigma\sqrt{2\,\pi}} \exp\left[\frac{-[\ln(k) - \mu^2]^2}{2\sigma^2}\right], \qquad (3)$$

which depends on the parameters $\mu \equiv \ln\left[\langle k\rangle^2/\sqrt{\langle k^2\rangle}\right]$ and $\sigma \equiv \sqrt{\ln\left[\langle k^2\rangle/\langle k\rangle^2\right]}$, where $\langle m\rangle = \sum_i k_i/N$ and k_i is the number of connections that node i has.

A comparison between the connectivity distributions of the SBQI and OFBQI highlights a few important differences. The OFBQI is governed by a Poissonian distribution, meaning that most of the nodes will have a connectivity close to $\langle m\rangle$, with deviations that become exponentially smaller as the network size increases [17]. On the contrary, the SBQI, being governed by a log-normal distribution, implies that there will be a non-negligible probability of finding nodes with a very high number of connections, which accounts for the fat-tail behavior seen in Fig. 2. That is, the SBQI leads to the existence of hubs, a characteristic trait of scale-free networks describing many networks [28–33]. For a long time, real-world networks have often been claimed to be scale free and thus governed by a power-law distribution. Recent works have shown robust evidence, however, that strongly scale-free structures are empirically rare: for most networks, log-normal

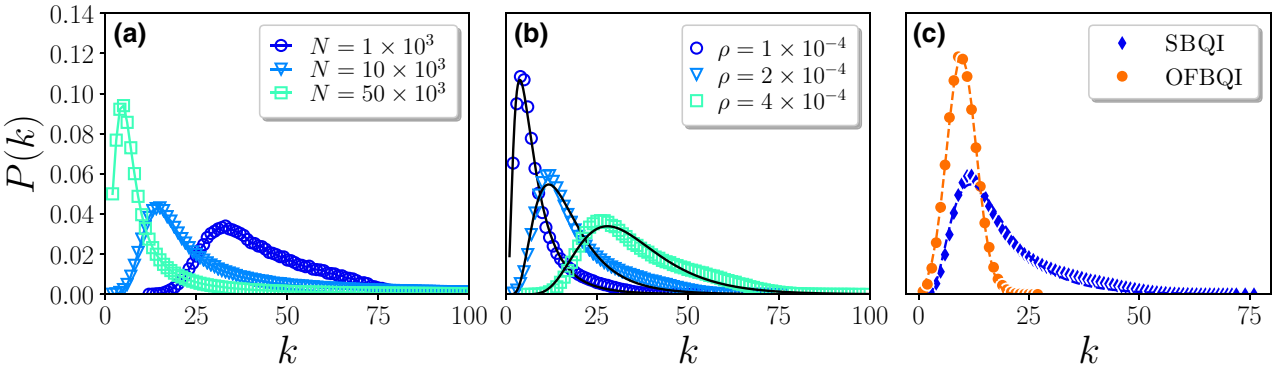

FIG. 2. The connectivity distribution of the SBQI model and a comparison with the OFBQI. The connectivity distribution of a SBQI model for (a) different values of N, setting $\rho = 5 \times 10^{-3}$ and (b) several values of ρ, setting $N = 1000$. The solid lines show the log-normal distribution (3) parametrized by μ and σ, fitting the distribution generated by the model almost perfectly. (c) A comparison between the satellite (red diamond) and the optical-fiber (blue circle) networks for $N = 1000$ and $\rho = 2 \times 10^{-4}$ ($R \simeq 1261$ km). The appearance of hubs in the satellite model becomes evident, according to the fat-tailed behavior. For the satellite model $n_p = 50$ and for the fiber one $n_p = 1000$, that is, we are allowing 20 times more photons for the optical-fiber model to establish a quantum link, an important advantage of the satellite implementation.

distributions fit the data as well or better than power laws [34].

We also note that it is intuitive to expect that the current model leads to a connectivity-distribution behavior that is in between the random networks (given by a Poissonian) and the scale-free networks (given by a power law). This is because, while in the first instance every pair of nodes has the same probability of receiving a connection, in the latter, nodes that have more links are more likely to receive more connections. However, in the current model, although there is no preferential attachment, the distance between the nodes and the satellite changes the probability of receiving links: the nodes lying below the satellite will naturally display more connections than those lying at the extremes of the satellite coverage area. Thus, although we expect the appearance of hubs, they will be highly concentrated in the central area.

A consequence of the existence of hubs is to decrease the typical network distance between nodes. This can be checked by looking at how the average shortest path $\langle l\rangle$ of the network (the averaging being performed over all pairs of nodes as well as over all samples of the networks) scales with the network size. To compute the average shortest path length $\langle l\rangle$, we use the standard definition in the network-science literature, given by

$$\langle l\rangle = \frac{2}{N(N-1)}\sum_{i<j} d_{ij},$$

where d_{ij} is the shortest path between sites i and j. Thus $\langle l\rangle$ is the average of the shortest paths between all pairs of nodes in the network. As is standard in the literature, we only compute $\langle l\rangle$ for the sites belonging to the giant cluster, once that $d_{ij} = \infty$ if i and j do not belong to the

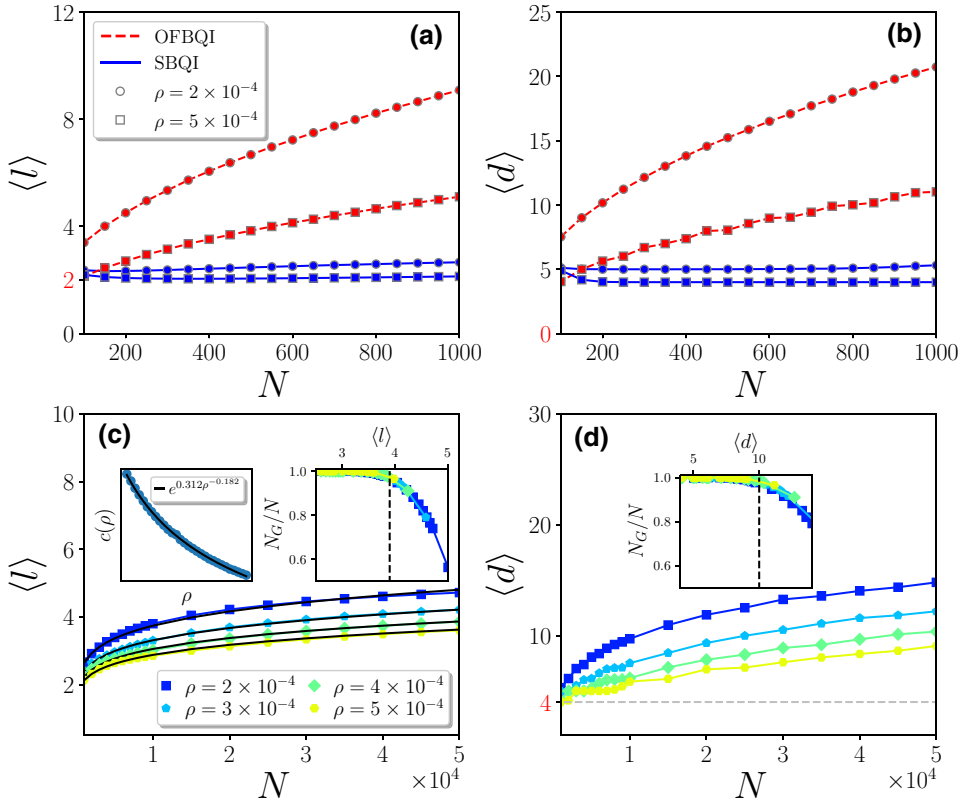

FIG. 3. A comparison between the SBQI and OFBQI networks. The average shortest path $\langle l\rangle$ and the average diameter $\langle d\rangle$ as a function of N for different values of $\rho \equiv N/\pi R^2$. Here, we are considering only the giant cluster, given that by definition two disconnected nodes have $\langle l\rangle = \infty$. (a) A comparison of $\langle l\rangle$ between OFBQI (red dashed line) and SBQI (blue straight line) for $\rho = 2.0(\times10^{-4})$ (circles) and $5.0(\times10^{-4})$ (squares). (b) A comparison of the diameter of the network $\langle d\rangle$ for the OFBQI and SBQI models, for the same parameters as before, once more highlights the advantage of the satellite model. (c),(d) It is shown that $\langle l\rangle$ and $\langle d\rangle$ remain small for the SBQI, even for very large N (also considering different density values ρ). The inset plots in (c) (right) and (d) show the relative size of the giant cluster as a function of the average shortest path and diameter, respectively. In the connected regime of the network ($N_G \sim N$), the shortest path is at most $\langle l\rangle_{\max} \sim 4$ and $\langle d\rangle_{\max} \sim 10$, independent of N and ρ. The black straight lines in Fig. 3(c) are given by the equation $c(\rho)\ln(N)/\ln(\langle k\rangle/\rho)$, with $c(\rho) = e^{0.312\rho^{-0.182}}$, and the dependence of $c(\rho)$ as a function of ρ is displayed in the left inset plot in (c).

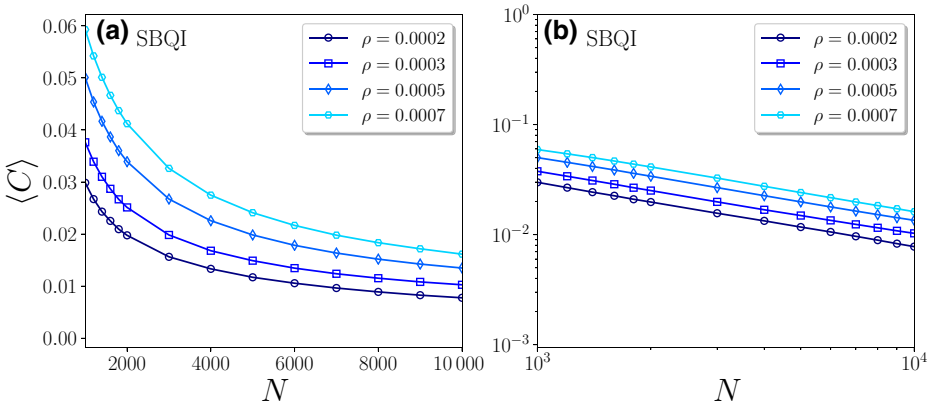

FIG. 4. The average clustering coefficient. (a) $\langle C \rangle$ for the SBQI model as a function of N for several values of ρ. (b) As can be seen, $\langle C \rangle$ decreases almost as a power of N. The simulations are run for 1000 realizations for each value of N, with $N_{\max} = 10\,000$. To be sure if $\langle C \rangle \sim N^{-\alpha}$, it would be necessary to run the simulations for higher values of N.

same subgraph. In a quantum network in the connected phase, any node can become entangled to any other node, via a entanglement swapping over the intermediate nodes. However, due to unavoidable noise, each of those intermediary processes damages the final amount of entanglement between the end nodes, highlighting the relevance of having a small $\langle l \rangle$. Efficient communication networks display the small-world property. Unfortunately, as shown in Ref. [17], the fiber-based quantum Internet displays no small-world property with $\langle l \rangle \sim \sqrt{N}$. Here, on the contrary, as shown in Fig. 3, $\langle l \rangle$ for the SBQI is governed by the functional $c(\rho) \ln N / \ln[\langle k \rangle / \rho]$, with $c(\rho) = e^{0.312\rho^{-0.182}}$. Thus, the satellite-based quantum networks display the small-world phenomenon. This property comes from the presence of hubs in the center of the network area that tend to shorten the path between any two nodes in the network. We also analyze the average clustering coefficient, defined by $\langle C \rangle = 1/N \sum_i c_i$, where c_i is the clustering coefficient of the site i given by $c_i = 2n_i/k_i(k_i - 1)$, in which n_i is the number of edges between the k_i neighbors of the site i and $k_i(k_i - 1)/2$ is the total possible number of edges between them. This property is a measure of the local link density, that is, of the degree of connectedness of the neighbors of a given site. Contrary to the traditional small-world model, proposed by Watts and Strogatz [18], and different from the OFBQI network, $\langle C \rangle^{\mathrm{SBQI}}$ decreases almost as a power of N (see Fig. 4). The small-world property ($\langle l \rangle \sim \log N$) with a decreasing clustering coefficient is also observed in the paradigmatic Erdos-Renyi [35] or Albert-Barabási [28] networks.

The satellite network also improves over the optical-fiber one when considering the diameter of the network (the greatest distance between any pair of nodes), $\langle d \rangle$. This quantity gives the maximum number of entanglement swaps needed in order to directly entangle any two nodes. As can be seen in Fig. 3(b), using a satellite as a quantum channel generates a final network with a considerably shorter diameter as compared to optical fibers. For instance, choosing $N = 1000$ and the coverage area as $R \approx 1260$ km, and even by setting $n_p^{\mathrm{OFBQI}} = 1000$ while $n_p^{\mathrm{SBQI}} = 50$, the diameter of the OFBQI network would be greater than in the SBQI case ($d_{\mathrm{OFBQI}} \sim 20$, $d_{\mathrm{SBQI}} \sim 4$).

In summary, using satellites and a small number of nodes, one can achieve a fully connected network covering very large areas and requiring few entanglement swaps to interconnect any two nodes, a clear advantage in the practical implementation of the quantum Internet.

IV. CONNECTIVITY OF THE QUANTUM INTERNET

Another relevant difference between the two models is that in the fiber model, the average connectivity depends linearly on the density of nodes $\rho = N/\pi R^2$ such that $\langle m \rangle = \alpha\rho$ [17]. We observe that for the SBQI, $\langle k \rangle$ has a much more intricate functional dependence, which is described well by

$$\langle k \rangle = \frac{A(\rho)}{\ln(\pi R^2)\sigma\sqrt{2\pi}} \exp\left[-\frac{[\ln\ln(\pi R^2) - \mu]^2}{2\sigma^2}\right], \quad (4)$$

where $A(\rho) \simeq 4.5 \times 10^5 \rho + 0.97$, $\mu \simeq 2.73$, and $\sigma \simeq 0.126$. To find the expression for $\langle k \rangle$, we generate the model by varying the parameters N and ρ and analyze how $\langle k \rangle$ changes with N, fixing ρ, and vice versa [see Figs. 5(a) and 5(b)]. By rescaling the axis of Fig. 5(a), we can find a universal behavior (data collapse) of $\langle k \rangle$. We fit the final data [Fig. 5(c)] and derive an expression for $\langle k \rangle$ that describes the simulation data very well. Interestingly, as can be seen in Fig. 5(a), $\langle k \rangle$ has a maximum value (peak), from which the curve decreases. Since ρ is fixed, by increasing N we also increase R. This means that when we increase N, we add nodes that are far from the satellite and will consequently receive fewer connections, leading to a decrease of $\langle k \rangle$.

For a communication network to be useful, it should have most of its nodes belonging to the same cluster and

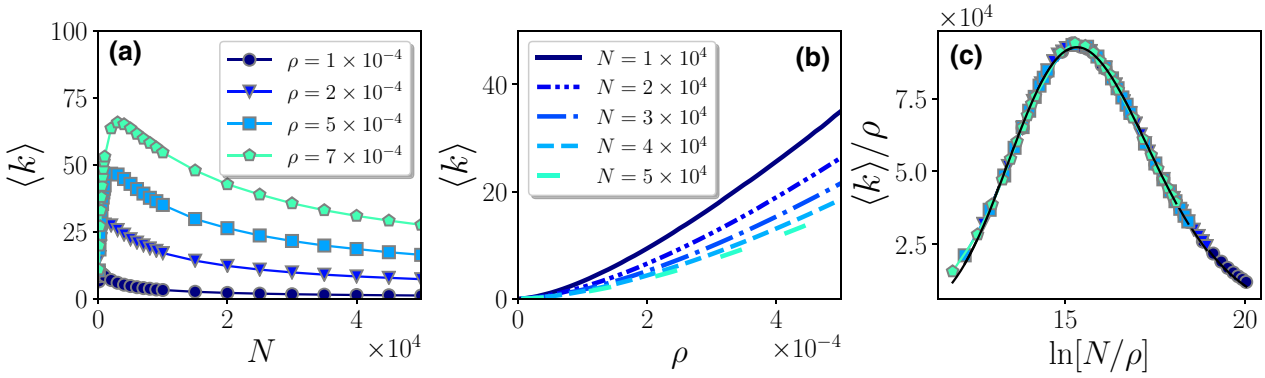

FIG. 5. The average degree of the network. (a),(b) $\langle k \rangle$ as a function of N and ρ, respectively. (c) Equation (4) (solid black line) fits the average degree very well, where by replacing $\langle k \rangle \to \langle k \rangle / \rho$ and $N \to \ln[N/\rho]$, all curves collapse, yielding a universal behavior that is independent of N and ρ.

not isolated in a few small-size clusters. In models such as the paradigmatic Erdos-Renyi random-network model [35] or the OFBQI [17], the emergence of the giant cluster is regulated by the average connectivity, such that this happens if $\langle m \rangle$ is above a critical value. As shown in Fig. 6, the SBQI also displays a transition from small disconnected clusters to a connected largest cluster.

Note that the SBQI model generates a connected network in large areas and still maintains a small average path. For instance, for $N = 1000$ and $n_p = 50$, the SBQI model generates a fully connected network ($N_G \sim N$), covering an area of radius $R \approx 1800$ km. With the same parameters, the OFBQI network would cover a maximum area of radius $R \approx 1100$ km.

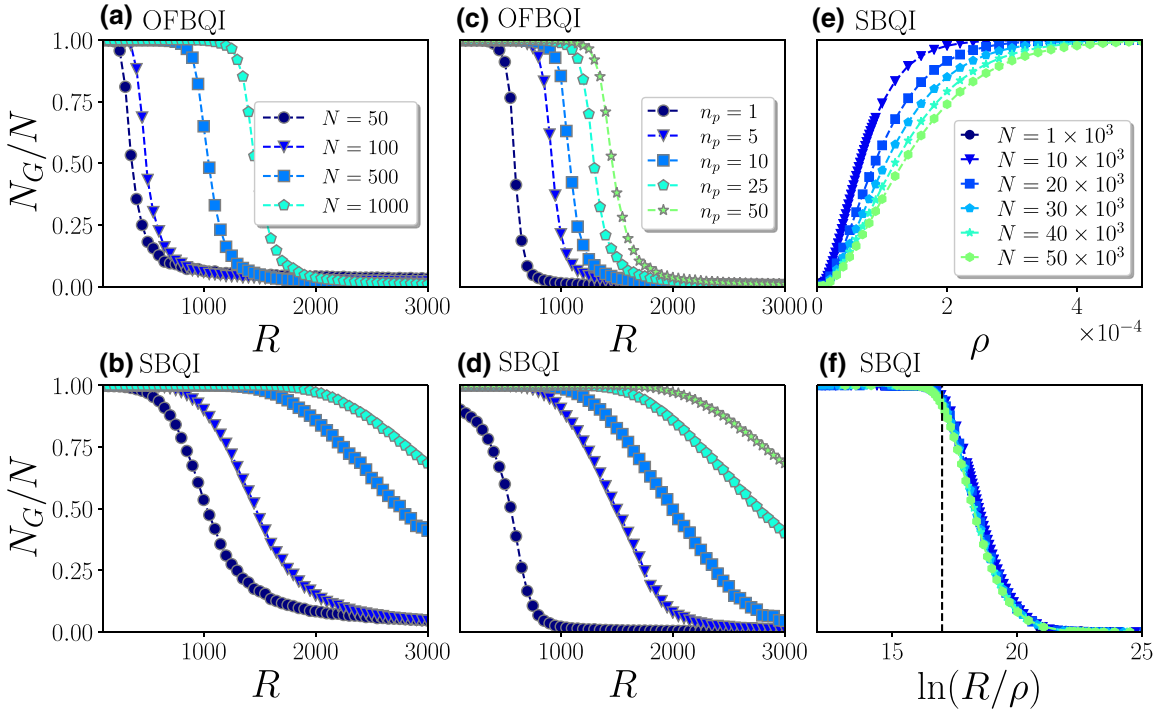

FIG. 6. The relative size of the giant cluster (N_G/N). A comparison between the (a) OFBQI and (b) SBQI models for $n_p = 50$ and $N = 50$, 100, 500, and 1000. A comparison between the (c) OFBQI and (d) SBQI models for $N = 1000$ and $n_p = 5$, 10, 25, and 50. Satisfactorily, the satellite network can be connected in very large areas, even with relatively small values of n_p and N. (e),(f) The transition between the disconnected and connected phases in the satellite model (for various values of N) as a function of ρ and $\ln(R/\rho)$, respectively. As can be seen in (f), the network remains connected ($N_G \sim N$) if $\ln(R/\rho) \lesssim 17$, which is equivalent to $\rho \gtrsim \left[e^{-17}\sqrt{N/\pi}\right]^{2/3}$, indicating that for each N, a density exists beyond which the network becomes connected.

V. ROBUSTNESS AGAINST FAILURES AND ATTACKS

Here, we analyze and compare the robustness of the satellite and optical-fiber models, considering the behavior of the networks under random failures and targeted attacks on nodes and links [24]. As a benchmark, we will also use the paradigmatic random [35] and scale-free networks [28]. If there is a random failure in a node, all of its connections are broken. Alternatively, one can think of a targeted attack breaking the nodes on the most connected sites of the network. Our goal is to determine how many nodes have to fail in a network in order for it to break apart.

To answer this, we need to compute the ratio $N_G(f)/N_G(0)$ as a function of f (the number of removed nodes divided by the size N of the network). The parameter $N_G(f)$ is the size of the giant cluster after we remove a fraction f of nodes from the network and $N_G(0)$ is the size of the largest cluster before any node removal. Analysis of this ratio as a function of f is the standard procedure in network science to obtain the robustness of the network under random failures (if we randomly remove the nodes) or targeted attacks (if we start removing the most connected nodes of the network) [23–25].

In Fig. 7, we show the average value of $N_G(f)/N_G(0)$, denoted by $\langle n_g \rangle$, for both random failures and targeted attacks. For random failures, the SBQI is significantly more robust than the OFBQI, as can be seen by comparing the critical values f_c (for which $\langle n_g \rangle$ is approximately zero) and the faster decay rate of the OFBQI. Furthermore, we can see that the SBQI has a similar behavior to a scale-free network, which is known to be robust against random failures [24,36].

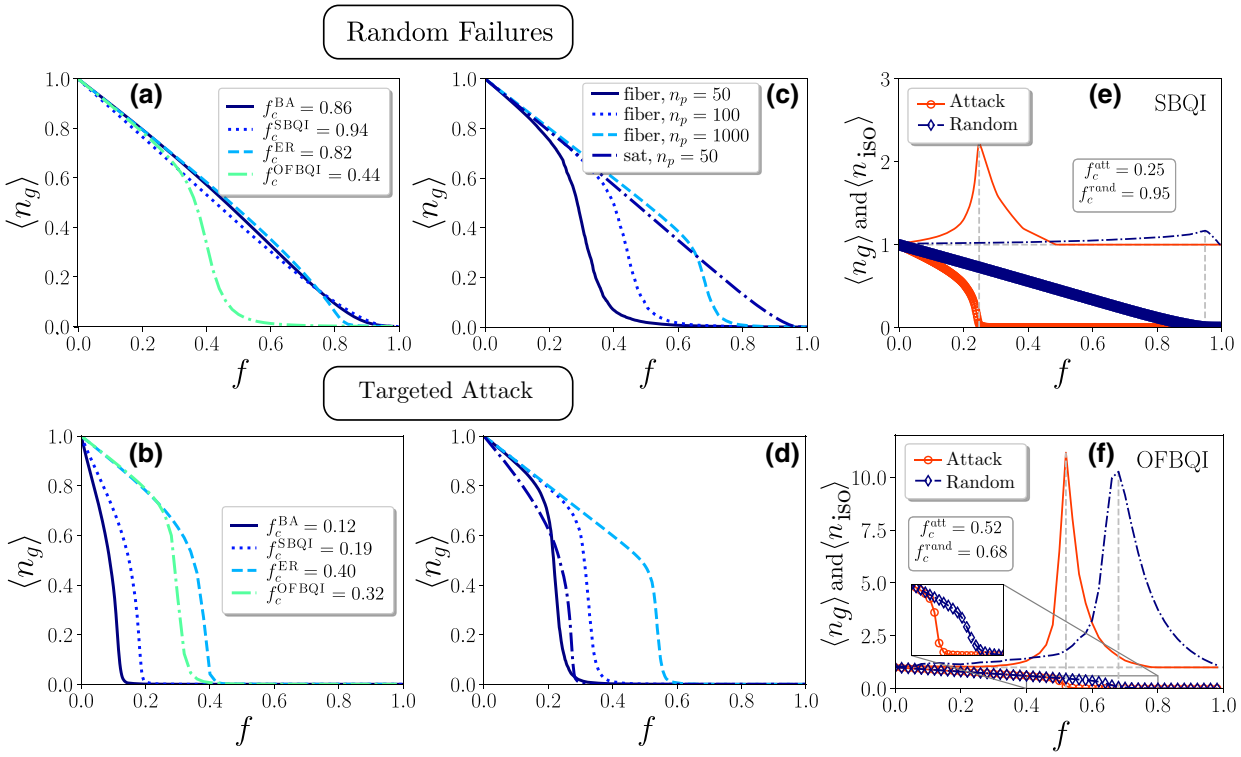

FIG. 7. Quantum network robustness. A comparison between the optical-fiber and satellite models, also having the Barabási-Albert (BA) (scale-free model) and the standard Erdos-Renyi random graph (ER) as benchmarks. We set $N = 10\,000$ and, as is standard in the literature, choose the parameters of each model to obtain a network with $\langle k \rangle \simeq 6$. (a) The SBQI is as robust as the BA model under random failures. The removal of 94% of the nodes is necessary to break the network. On the other hand, the OFBQI is the least robust network. (b) As expected, the ER model is the most robust under targeted attacks, with $f_c \sim 40\%$, followed by the OFBQI with $f_c = 32\%$. The least robust is the BA ($f_c \sim 12\%$), which is similar to the SBQI model with $f_c \sim 19\%$. (c),(d) A comparison between the fiber and satellite models fixing $N = 10\,000$ and $\rho = 0.00022$ sites per kilometer, varying $n_p = 50$, 100, and 1000 for the OFBQI network and fixing $n_p = 50$ for the SBQI model. Even allowing for considerably greater losses, the OFBQI is less robust than the SBQI network under random failures and it becomes less robust as n_p decreases. However, the SBQI model is very fragile against targeted attacks, while the OFBQI becomes more robust for larger values of n_p (e.g., $n_p \geq 100$). (e)–(f) The critical threshold f_c for the SBQI and the OFBQI under random failures and targeted attacks, fixing $\rho = 0.0002$ sites per kilometer: (e) the SBQI, with $n_p = 50$, and (f) the OFBQI, with $n_p = 1000$, under random failures (blue) and targeted attacks (red). We compare $\langle n_g \rangle$ [blue diamonds (red circles)] with $\langle n_{iso} \rangle$ [blue dashed-dotted line (red straight line)] as a function of the fraction f of removed nodes under random failures (targeted attacks). The peak of the $\langle n_{iso} \rangle$ coincides with $\langle n_g \rangle \sim 0$, indicating the value of the critical threshold f_c.

Due to the existence of hubs, it is well known that the scale-free model is less robust against targeted attacks as compared, for instance, with random networks. In the SBQI, such hubs are also present and, as shown in Fig. 7, this leads to a smaller degree of robustness in this situation.

An alternative method to obtain the critical threshold f_c is to compare $\langle n_g \rangle$ with the average size of the isolated clusters $\langle n_{\rm iso} \rangle$ as a function of the fraction f of removed nodes [24]. As shown in Figs. 7(e) and 7(f), the peak of $\langle n_{\rm iso} \rangle$ coincides with $\langle n_g \rangle \sim 0$, indicating the value of the critical threshold f_c. From this point on, the network loses its communication capacity. As can be seen in Fig. 7(f), under random failures, a failure of 68% of nodes is enough to bring down the communication capabilities of the OFBQI network, whereas for the SBQI network [Fig. 7(e)], almost all of the nodes of the network (approximately 95%) would have to fail in order for it to break down. In turn, under targeted attacks, the failure of only about 25% of the nodes would already be enough to break the SBQI network [Fig. 7(e)], while for the OFBQI it is necessary that about 52% of the nodes fail [Fig. 7(f)].

We also study two cases of link failure: (1) random link failures and (2) "edge-cut" attacks. Note that the first kind of failure would correspond to the sources of noise (decoherence etc.) and the second kind would correspond to an attack that specifically chooses the links necessary to break down all the paths between two nodes (breaking off the communication between them). In Figs. 8(a) and 8(b), we fix the parameters $\rho = 0.0002$ sites per kilometer and $N = 10\,000$ under 1000 realizations and we show the robustness of the (a) SBQI and (b) OFBQI models under random link failures. By comparing the random link failure with the case of the random node failure, we can see that for the SBQI network, the critical thresholds f_c are equivalent. This result is known for networks where the probability of linking two sites does not strongly depend on the distance between them (e.g., the Erdos-Renyi [35] and Barabási-Albert [28] networks). As discussed, in the SBQI model, the distance between the sites is almost irrelevant with regard to the link probability, which explains this result. On the contrary, the OFBQI model displays higher robustness under random link failures as compared to node failures. In conclusion, for random link failures also, the SBQI is still much more robust than the OFBQI.

In the second case, shown in Figs. 8(c) and 8(d) ("edge-cut" attack), we compare the networks by removing the minimum number of links necessary to fully disconnect two randomly chosen nodes. As can be seen in Figs. 8(c) (SBQI) and 8(d) (OFBQI), under this kind of attack, the SBQI model is again more robust than the OFBQI model. We can see in Fig. 8(c) that there is no critical threshold beyond which $N_G/N = 0$ and the network becomes disconnected. However, the OFBQI network becomes more fragile under this kind of attack.

In summary, under link failures, the SBQI is again more robust than the OFBQI. We must point out, however, that the results regarding link failures are preliminary. The bottleneck of the analysis is the computational cost of considering very large networks. For this reason, we consider a relatively small N as compared to the node-failure case.

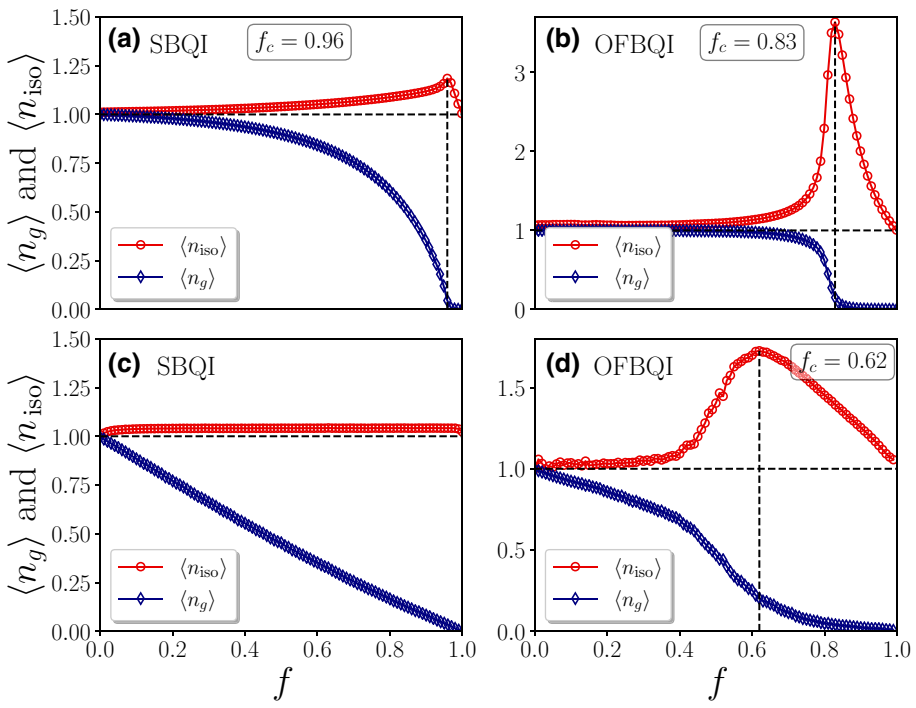

FIG. 8. Robustness under link removal. In these figures, we show the robustness of the (a) SBQI and (b) the OFBQI under random link failures. The results are obtained for $\rho = 0.0002$ and $N = 10\,000$ under 1000 realizations. Below, we show the robustness of the models, (c) SBQI and (d) OFBQI, by removing the minimum number of links necessary to break the communication between two randomly chosen nodes. The results are obtained for $\rho = 0.0002$ sites per kilometer and $N = 1000$ under 1000 realizations. In both cases, the SBQI is more robust than OFBQI network.

VI. DISCUSSION AND CONCLUSIONS

We study the network properties of a quantum Internet, assuming that the links interconnecting the different nodes are quantum channels mediated by a satellite with downlink communication with stations on the ground. We show that such networks display hubs, i.e.,, nodes that have a large number of connections, naturally present closer to the satellite. These nodes have the effect of making the typical network distances and diameter small. This leads to a clear advantage of such networks in entanglement distribution, as compared to networks based on optical fibers [17]. The presence of hubs also makes the network more robust against random node and link failures, since these nodes also have the capability to hold the network together after a considerable number of nodes are removed. However, if the attacks are targeted to destroy the hubs, the network is dismantled pretty easily. This highlights the need for special protection of these nodes.

Our results provide a useful guide for the development of future quantum networks. Together with the network based on optical fibers [17], our results can be seen as the first step toward more complicated and realistic models. It would be interesting to consider a nonuniform distribution of nodes that, for instance, simulates the fact that big cities typically have a greater concentration of nodes than rural areas. We expect that this situation could lead to the appearance of communities. Other important lines of research could be to study quantum features of the transmitted photons, such as coherence and entanglement, and how these features impact the usefulness of the network for specific protocols. Finally, we believe that future quantum networks will be hybrid, simultaneously using optical fibers and satellites in the most efficient way.

ACKNOWLEDGMENTS

We acknowledge the John Templeton Foundation via the "Causality in the quantum world: Harnessing quantum effects in causal inference problems" (Q-CAUSAL) Grant No. 61084, the Serrapilheira Institute (Grant No. Serra-1708-15763), the Brazilian National Council for Scientific and Technological Development (CNPq) via the National Institute for Science and Technology on Quantum Information (INCT-IQ) and Grants No. 423713/2016-7, No. 307172/2017-1, and No. 406574/2018-9, and the Brazilian Ministry of Science, Technology, Innovations, and Communications (MCTIC) and Ministry of Education (MEC). DC acknowledges the Ramon y Cajal fellowship, the Government of Spain (FIS2020-TRANQI and Severo Ochoa CEX2019-000910-S), Fundació Cellex, Fundació Mir-Puig, Generalitat de Catalunya (CERCA, AGAUR SGR 1381), ERC AdG CERQUTE. A.C. acknowledges the Universidade Federal de Alagoas (UFAL) for a paid license for scientific cooperation at the Federal University of Rio Grande do Norte (UFRN). We thank the High Performance Computing Center (NPAD/UFRN) for providing computational resources.

[1] Charles H. Bennett and Stephen J. Wiesner, Communication via One- and Two-Particle Operators on Einstein-Podolsky-Rosen States, Phys. Rev. Lett. **69**, 2881 (1992).
[2] Nicolas Gisin, Grégoire Ribordy, Wolfgang Tittel, and Hugo Zbinden, Quantum cryptography, Rev. Mod. Phys. **74**, 145 (2002).
[3] Charles H. Bennett, Gilles Brassard, Claude Crépeau, Richard Jozsa, Asher Peres, and William K. Wootters, Teleporting an Unknown Quantum State via Dual Classical and Einstein-Podolsky-Rosen Channels, Phys. Rev. Lett. **70**, 1895 (1993).
[4] Nicolas Brunner, Daniel Cavalcanti, Stefano Pironio, Valerio Scarani, and Stephanie Wehner, Bell nonlocality, Rev. Mod. Phys. **86**, 419 (2014).
[5] P. Kómár, E. M. Kessler, M. Bishof, L. Jiang, A. S. Sorensen, J. Ye, and M. D. Lukin, A quantum network of clocks, Nat. Phys. **10**, 582 EP (2014).
[6] Anne Broadbent, Joseph Fitzsimons, and Elham Kashefi, in 2009 50th Annual IEEE Symposium on Foundations of Computer Science (IEEE, New York, 2009).
[7] Joseph F. Fitzsimons and Elham Kashefi, Unconditionally verifiable blind quantum computation, Phys. Rev. A **96**, 012303 (2017).
[8] Christoph Simon, Towards a global quantum network, Nat. Photonics **11**, 678 (2017).
[9] Raju Valivarthi, Qiang Zhou, Gabriel H. Aguilar, Varun B. Verma, Francesco Marsili, Matthew D. Shaw, Sae Woo Nam, Daniel Oblak, and Wolfgang Tittel *et al.*, Quantum teleportation across a metropolitan fibre network, Nat. Photonics **10**, 676 (2016).
[10] Sören Wengerowsky, Siddarth Koduru Joshi, Fabian Steinlechner, Julien R. Zichi, Sergiy M. Dobrovolskiy, René van der Molen, Johannes W. N. Los, Val Zwiller, Marijn A. M. Versteegh, and Alberto Mura *et al.*, Entanglement distribution over a 96-km-long submarine optical fiber, Proc. Natl. Acad. Sci. **116**, 6684 (2019).
[11] Robert Bedington, Juan Miguel Arrazola, and Alexander Ling, Progress in satellite quantum key distribution, Npj Quantum Inf. **3**, 30 (2017).
[12] Juan Yin *et al.*, Satellite-based entanglement distribution over 1200 kilometers, Science **356**, 1140 (2017).
[13] Sheng-Kai Liao *et al.*, Satellite-Relayed Intercontinental Quantum Network, Phys. Rev. Lett. **120**, 030501 (2018).
[14] H. Jeff Kimble, The quantum Internet, Nature **453**, 1023 (2008).
[15] Stephanie Wehner, David Elkouss, and Ronald Hanson, Quantum Internet: A vision for the road ahead, Science **362**, eaam9288 (2018).
[16] Liang Huang and Ying-Cheng Lai, Cascading dynamics in complex quantum networks, Chaos: Interdiscip. J. Nonlinear Sci. **21**, 025107 (2011).
[17] Samuraí Brito, Askery Canabarro, Rafael Chaves, and Daniel Cavalcanti, Statistical Properties of the Quantum Internet, Phys. Rev. Lett. **124**, 210501 (2020).

[18] Duncan J. Watts and Steven H. Strogatz, Collective dynamics of "small-world" networks, Nature **393**, 440 (1998).
[19] Marc Barthélémy and Luís A. Nunes Amaral, Small-World Networks: Evidence for a Crossover Picture, Phys. Rev. Lett. **82**, 3180 (1999).
[20] Lidia A. Braunstein, Sergey V. Buldyrev, Reuven Cohen, Shlomo Havlin, and H. Eugene Stanley, Optimal Paths in Disordered Complex Networks, Phys. Rev. Lett. **91**, 168701 (2003).
[21] Mark D. Humphries and Kevin Gurney, Network "small-world-ness": A quantitative method for determining canonical network equivalence, PLoS ONE **3**, e0002051 (2008).
[22] ZACHARY P. NEAL, How small is it? comparing indices of small worldliness, Netw. Sci. **5**, 30 (2017).
[23] Albert-László Barabási *et al.*, *Network Science* (Cambridge University Press, Cambridge, England, 2016).
[24] Réka Albert, Hawoong Jeong, and Albert-László Barabási, Error and attack tolerance of complex networks, Nature **406**, 378 (2000).
[25] Reuven Cohen, Keren Erez, Daniel ben Avraham, and Shlomo Havlin, Resilience of the Internet to Random Breakdowns, Phys. Rev. Lett. **85**, 4626 (2000).
[26] C. Bonato, A. Tomaello, V. Da Deppo, G. Naletto, and P. Villoresi, Feasibility of satellite quantum key distribution, New J. Phys. **11**, 045017 (2009).
[27] Elizabeth Gibney, One giant step for quantum Internet, Nature **535**, 478 (2016).
[28] Réka Albert, Hawoong Jeong, and Albert-László Barabási, Diameter of the World-Wide Web, Nature **401**, 130 (1999).
[29] Albert-László Barabási and Eric Bonabeau, Scale-free networks, Sci. Am. **288**, 60 (2003).
[30] Michalis Faloutsos, Petros Faloutsos, and Christos Faloutsos, On power-law relationships of the Internet topology, SIGCOMM Comput. Commun. Rev. **29**, 251 (1999).
[31] S. Redner, How popular is your paper? an empirical study of the citation distribution, Eur. Phys. J. B—Condens. Matter Complex Syst. **4**, 131 (1998).
[32] H. Jeong, B. Tombor, R. Albert, Z. N. Oltvai, and A.-L. Barabási, The large-scale organization of metabolic networks, Nature **407**, 651 (2000).
[33] Soon-Hyung Yook, Hawoong Jeong, and Albert-László Barabási, Modeling the Internet's large-scale topology, Proc. Natl. Acad. Sci. **99**, 13382 (2002).
[34] Anna D. Broido and Aaron Clauset, Scale-free networks are rare, Nat. Commun. **10**, 1017 (2019).
[35] Paul Erdos and Alfréd Rényi, On random graphs, Publ. Math. Debrecen **6**, 290 (1959).
[36] Hidefumi Sawai, A small-world network immune from random failures and resilient to targeted attacks, Procedia Comput. Sci. **18**, 976 (2013).